Journal of Applied Analysis and Computation
Volume 7, Number 1, February 2017, 278–290
Website:http://jaac-online.com/
DOI:10.11948/2017019

PLANAR BIFURCATION METHOD OF DYNAMICAL SYSTEM FOR INVESTIGATING DIFFERENT KINDS OF BOUNDED TRAVELLING WAVE SOLUTIONS OF A GENERALIZED CAMASSA-HOLM EQUATION*

Shaolong Xie[1], Xiaochun Hong[2,†] and Tao Jiang[3]

Abstract In this study, by using planar bifurcation method of dynamical system, we study a generalized Camassa-Holm (gCH) equation. As results, under different parameter conditions, many bounded travelling wave solutions such as periodic waves, periodic cusp waves, solitary waves, peakons, loops and kink waves are given. The dynamic properties of these exact solutions are investigated.

Keywords GCH equation, periodic wave, periodic cusp wave, peakon, loop, kink wave.

MSC(2010) 35B10, 35C07, 35C08.

1. Introduction

In recent years, there has been a growing interest in integrable non-evolutionary partial differential equations of the form [7, 9, 10]

$$\left(1-D_x^2\right)u_t=F\left(u,u_x,u_{xx},u_{xxx},\cdots\right), \tag{1.1}$$

where $u=u(x,t)$, $D_x=\frac{\partial}{\partial x}$, F is expressed by some functions of u and its derivatives with respect to x. The most celebrated example of this type of (1.1) is the following Camassa-Holm equation [4]

$$\left(1-D_x^2\right)u_t=-2ku_x-3uu_x+2u_xu_{xx}+uu_{xxx}. \tag{1.2}$$

This equation (1.2) has attracted much researchers in recent years both from analytical and numerical point of view, see the references [1, 2, 5, 6, 8, 13, 14, 16, 17, 20–23] and the references cited therein. For $k=0$, Camassa and Holm showed that Eq. (1.2) has peakons of the form $u(x,t)=ce^{-|x-ct|}$. In the fields of mathematics and physics, a soliton is a solitary wave with packet or pulse that maintains its shape while traveling at constant speed. This type of wave has been the focus interest since solitons are thus stable, and do not disperse over time. Peakon is a type of non-smooth soliton, discovered by Camassa and Holm; the wave has a sharp peak

†the corresponding author. Email address: xchong@ynufe.edu.cn(X. Hong)
[1]Business School, Yuxi Normal University, 653100 Yuxi, China
[2]School of Statistics and Mathematics, Yunnan University of Finance and Economics, 650221 Kunming, China
[3]School of Information, Beijing Wuzi University, 101149 Beijing, China
*The authors were supported by National Natural Science Foundation of China (No. 11161038).

where it has not derivative at the peak point. The wave profile is similar to the graph of the function $e^{|x|}$.

More recently, Novikov [15] and Mikhailov and Novikov [16] showed that there are other examples of NLPDEs in the class of Eq. (1.1) which are integrable. Novikov presented a detailed summary of integrable and homogeneous polynomial generalizations of the Camass-Holm type equation with quadratic and cubic nonlinearities.

In this study, by using the planar bifurcation method of dynamical system [11, 12], we will study different kinds of bounded travelling wave solutions and dynamical behaviors of the following a generalized Camassa-Holm (gCH) equation [16]

$$\left(1-D_x^2\right)u_t = D_x\left(4-D_x^2\right)u^2. \tag{1.3}$$

The exact representation of bounded travelling wave solutions of the gCH are obtained. the planar graphs of the travelling wave solutions is shown under some parameters. These results are not in [19].

The rest of this study is organized as follows. In Section 2, we will derive travelling wave solutions. In Section 3, we will give classifications of travelling wave solutions of (1.3), and make numerical simulations of some bounded travelling wave by using mathematical software. Finally, a short conclusion is given in Section 4.

2. Travelling wave solutions

Making the transformation $u(x,t)=\varphi(\xi)$ with $\xi = x - ct$, the equation (1.3) can be reduced to the following ordinary differential equation:

$$2\varphi\varphi''' + c\varphi''' + 6\varphi'\varphi'' - 8\varphi\varphi' - c\varphi' = 0, \tag{2.1}$$

where c is the wave speed, and the sign "$'$" is the derivative with respect to ξ.

Integrating (2.1) with respect to ξ, we have the following travelling wave equation,

$$(c+2\varphi)\varphi'' + 2\varphi'^2 - 4\varphi^2 - c\varphi = g, \tag{2.2}$$

where g is integration constant.

In (2.2), multiplying by $2(c+2\varphi)\varphi'$ on both sides of equation and then integrating it, we have

$$(c+2\varphi)^2\left(\frac{d\varphi}{d\xi}\right)^2 = 4\varphi^4 + 4c\varphi^3 + \left(2g+c^2\right)\varphi^2 + 2cg\varphi + h, \tag{2.3}$$

where h is integration constant. Let

$$d\xi = (c+2\varphi)d\tau, \tag{2.4}$$

then (2.3) becomes

$$\left(\frac{d\varphi}{d\tau}\right)^2 = 4\varphi^4 + 4c\varphi^3 + \left(2g+c^2\right)\varphi^2 + 2cg\varphi + h. \tag{2.5}$$

Let

$$f_0(\varphi) = 4\varphi^4 + 4c\varphi^3 + \left(2g+c^2\right)\varphi^2 + 2cg\varphi, \tag{2.6}$$

then

$$f_0'(\varphi) = 16\varphi^3 + 12c\varphi^2 + 2\left(2g + c^2\right)\varphi + 2cg. \tag{2.7}$$

Write

$$g_1(c) = \frac{c^2}{16}, \tag{2.8}$$

and

$$g_2(c) = -\frac{c^2}{2}. \tag{2.9}$$

Clearly, $f_0(\varphi)$ has three extreme points $\varphi_c = -\frac{c}{2}$ and $\varphi_\pm = \frac{-c\pm\sqrt{c^2-16g}}{8}$ when $g < g_1(c)$ and $g \neq g_2(c)$, a extreme point φ_c when $g \geq g_1(c)$, a extreme point φ_+ when $c > 0, g < g_1(c)$ and $g = g_2(c)$, a extreme point φ_- when $c < 0, g < g_1(c)$ and $g = g_2(c)$. Thus, we have some results as follows:

(1) If $g_1 \leq g$, then φ_c is a minimum point.

(2) If $c > 0, g_2 < g < g_1$, then φ_+ and φ_c are two minimum points and φ_- is a maximum point, and $\varphi_c < \varphi_- < \varphi_+$, and (2a) $f_0(\varphi_c) < f_0(\varphi_+) < f_0(\varphi_-)$ when $0 < g < g_1$, (2b) $f_0(\varphi_c) = f_0(\varphi_+) < f_0(\varphi_-)$ when $g = 0$, (2c) $f_0(\varphi_+) < f_0(\varphi_c) < f_0(\varphi_-)$ when $g_2 < g < 0$.

(3) If $c < 0, g_2 < g < g_1$, then φ_- and φ_c are two minimum points and φ_+ is a maximum point, and $\varphi_- < \varphi_+ < \varphi_c$, and (3a) $f_0(\varphi_c) < f_0(\varphi_-) < f_0(\varphi_+)$ when $0 < g < g_1$, (3b) $f_0(\varphi_-) = f_0(\varphi_c) < f_0(\varphi_+)$ when $g = 0$, (3c) $f_0(\varphi_-) < f_0(\varphi_c) < f_0(\varphi_+)$ when $g_2 < g < 0$.

(4) If $g = g_2$, then φ_+ is a minimum point when $c > 0$, φ_- is a minimum point when $c < 0$.

(5) If $g < g_2$, then φ_- and φ_+ are two minimum points and φ_c is a maximum point, and $\varphi_- < \varphi_c < \varphi_+$, and (5a) $f_0(\varphi_+) < f_0(\varphi_-) < f_0(\varphi_c)$ when $0 < c$, (5b) $f_0(\varphi_-) = f_0(\varphi_+) < f_0(\varphi_c)$ when $c = 0$, (5c) $f_0(\varphi_-) < f_0(\varphi_+) < f_0(\varphi_c)$ when $c < 0$.

Let

$$f(\varphi) = f_0(\varphi) + h, \tag{2.10}$$

then (2.3) and (2.5) can be rewritten as

$$\left(\frac{d\varphi}{d\xi}\right)^2 = \frac{f(\varphi)}{(c + 2\varphi)^2}, \tag{2.11}$$

and

$$\left(\frac{d\varphi}{d\tau}\right)^2 = f(\varphi). \tag{2.12}$$

2.1. Case of four real roots of $f(\varphi) = 0$

When the equation $f(\varphi) = 0$ have four real roots φ_i $(i = 1, 2, 3, 4)$, and $\varphi_1 < \varphi_2 < \varphi_3 < \varphi_4$, then

$$f(\varphi) = 4(\varphi - \varphi_1)(\varphi - \varphi_2)(\varphi - \varphi_3)(\varphi - \varphi_4). \tag{2.13}$$

Under the intervals $[\varphi_2,\ \varphi_3]$, substituting (2.13) into (2.12) to integrate via the formula 254.00 in [3], we get

$$\varphi = \varphi_1 + \frac{\varphi_2 - \varphi_1}{1 - \alpha^2 \mathrm{sn}^2(w, j)}, \tag{2.14}$$

where $w=\sqrt{(\varphi_4-\varphi_2)(\varphi_3-\varphi_1)}\tau$ is a parameter variable, $j=\sqrt{\frac{(\varphi_3-\varphi_2)(\varphi_4-\varphi_1)}{(\varphi_4-\varphi_2)(\varphi_3-\varphi_1)}}$ is the modulus of Jacobian elliptic function and $\alpha=\sqrt{\frac{\varphi_3-\varphi_2}{\varphi_3-\varphi_1}}$. Using formula 400.01 in [3], substituting (2.14) into (2.4) to integrate it, we get

$$\xi=\frac{1}{\sqrt{(\varphi_4-\varphi_2)(\varphi_3-\varphi_1)}}\left\{(c+2\varphi_1)w+2(\varphi_2-\varphi_1)\Pi\left[\mathrm{am}(w,j),\alpha^2,j\right]\right\}. \tag{2.15}$$

Thus we obtain a parametric form of solution of (1.3) as follows:

$$\begin{cases}\varphi=\varphi_1+\frac{\varphi_2-\varphi_1}{1-\alpha^2\mathrm{sn}^2(w,j)},\\ \xi=\frac{1}{\sqrt{(\varphi_4-\varphi_2)(\varphi_3-\varphi_1)}}\left\{(c+2\varphi_1)w+2(\varphi_2-\varphi_1)\Pi\left[\mathrm{am}(w,j),\alpha^2,j\right]\right\}.\end{cases} \tag{2.16}$$

2.2. Cases of one double and two real roots of $f(\varphi)=0$

(1) When φ_1 is a double root, φ_2 and φ_3 are two simple real roots of $f(\varphi)=0$, then

$$f(\varphi)=4(\varphi-\varphi_1)^2(\varphi-\varphi_2)(\varphi-\varphi_3), \tag{2.17}$$

where $\varphi_1<\varphi_2<\varphi_3$, the interval of integration is between the roots φ_1 and φ_2. Similarly, we obtain a parametric form of solution of (1.3) as follows:

$$\begin{cases}\varphi=\varphi_1+\dfrac{2(\varphi_2-\varphi_1)(\varphi_3-\varphi_1)}{\varphi_2+\varphi_3-2\varphi_1+(\varphi_3-\varphi_2)\cosh w},\\ \xi=\dfrac{1}{2\sqrt{(\varphi_2-\varphi_1)(\varphi_3-\varphi_1)}}\Bigg[(c+2\varphi_1)w+4\sqrt{(\varphi_2-\varphi_1)(\varphi_3-\varphi_1)}\\ \qquad\times\tanh^{-1}\left(\sqrt{\dfrac{\varphi_2-\varphi_1}{\varphi_3-\varphi_1}}\tanh\dfrac{w}{2}\right)\Bigg],\end{cases} \tag{2.18}$$

where $w=2\sqrt{(\varphi_2-\varphi_1)(\varphi_3-\varphi_1)}\tau$ is a parameter variable. Especially, when $\varphi_1=\varphi_c$, (2.18) becomes an explicit expression of solution as follows:

$$\varphi=\frac{1}{2}\left[\varphi_2+\varphi_3-(\varphi_3-\varphi_2)\cosh\xi\right]. \tag{2.19}$$

(2) When φ_1 and φ_2 are two simple real roots, φ_3 is a double root of $f(\varphi)=0$, then

$$f(\varphi)=4(\varphi-\varphi_1)(\varphi-\varphi_2)(\varphi-\varphi_3)^2, \tag{2.20}$$

where $\varphi_1<\varphi_2<\varphi_3$, the interval of integration is between the roots φ_2 and φ_3. Substituting (2.20) into (2.12) to integrate, we obtain a parametric form of solution of (1.3) as follows:

$$\begin{cases}\varphi=\varphi_3-\dfrac{2(\varphi_3-\varphi_1)(\varphi_3-\varphi_2)}{2\varphi_3-\varphi_1-\varphi_2+(\varphi_2-\varphi_1)\cosh w},\\ \xi=\dfrac{1}{2\sqrt{(\varphi_3-\varphi_1)(\varphi_3-\varphi_2)}}\Bigg[(c+2\varphi_3)w-4\sqrt{(\varphi_3-\varphi_1)(\varphi_3-\varphi_2)}\\ \qquad\times\tanh^{-1}\left(\sqrt{\dfrac{\varphi_3-\varphi_2}{\varphi_3-\varphi_1}}\tanh\dfrac{w}{2}\right)\Bigg],\end{cases} \tag{2.21}$$

where $w=2\sqrt{(\varphi_3-\varphi_1)(\varphi_3-\varphi_2)}\tau$ is a parameter variable. Especially, when $\varphi_3=\varphi_c$, (2.20) becomes an explicit expression of solution as follows:

$$\varphi=\frac{1}{2}\left[\varphi_1+\varphi_2+(\varphi_2-\varphi_1)\cosh\xi\right]. \tag{2.22}$$

2.3. Cases of two double real roots of $f(\varphi) = 0$

(i) When $g = 0$, $c \neq 0$ and $h = 0$, the φ_c and 0 are two double real roots of $f(\varphi) = 0$, then we have

$$f(\varphi) = 4(\varphi - \varphi_c)^2\varphi^2. \tag{2.23}$$

Substituting into (2.11) to integrate, we obtain a peakon solution of (1.3) as follows:

$$\varphi = \varphi_c \exp(-|\xi|). \tag{2.24}$$

(ii) When $g < 0$, $c = 0$ and $h = f(\varphi_-) = f(\varphi_+)$, the φ_- and φ_+ are two double real roots of $f(\varphi) = 0$ then $f(\varphi) = 4(\varphi - \varphi_-)^2(\varphi - \varphi_+)^2$, where $\varphi_- < \varphi_+$. Similarly, we obtain a peakon solution of (1.3) as follows:

$$(\varphi_+ - \varphi)^{\varphi_+}(\varphi - \varphi_-)^{-\varphi_-} = \varphi_+^{\varphi_+}(-\varphi_-)^{-\varphi_-} \exp\left[(\varphi_- - \varphi_+)|\xi|\right]. \tag{2.25}$$

3. Classifications of travelling wave solutions of Eq. (1.3)

Let $\frac{d\varphi}{d\xi} = z$, then $\frac{d\varphi}{d\tau} = (c + 2\varphi)z$, Eq. (2.2) becomes the following two dimensional system,

$$\begin{cases} \dfrac{d\varphi}{d\tau} = (c + 2\varphi)z, \\ \dfrac{dz}{d\tau} = 4\varphi^2 + c\varphi + g - 2z^2. \end{cases} \tag{3.1}$$

From the theory of the planar dynamical system, we know that the singular points of system (3.1) have following properties.

(1) When $g > g_2$, then $(\varphi_c, z_\pm)$ are two saddle points, where $z_\pm = \sqrt{\frac{c^2+2g}{4}}$.

(2) When $g = g_1$, then $\varphi_- = \varphi_+ = -\frac{c}{8}$, $\left(0, -\frac{c}{8}\right)$ is a degenerate saddle point.

(3) When $g_2 < g < g_1$, and $c > 0$, then $(\varphi_-, 0)$ is a center point, $(\varphi_+, 0)$ is a saddle point.

(4) When $g_2 < g < g_1$, and $c < 0$, then $(\varphi_+, 0)$ is a center point, $(\varphi_-, 0)$ is a saddle point.

(5) If $g = g_2$, then $(0, \varphi_c)$ is a degenerate saddle point, $(0, \varphi_-)$ a saddle point when $c < 0$, $(0, \varphi_+)$ is a saddle point when $c > 0$.

(6) When $g < g_2$, then $(0, \varphi_\pm)$ are two saddle points.

Using the bifurcation method of planar systems, as [11], in different regions parameter plane, we draw the bifurcation phase portraits of Eq. (1.3) which are shown in Figures 1, 2 and 3.

Based on the above analysis, we obtain the classification of the travelling wave solutions of Eq. (1.3).

3.1. Smooth periodic wave

Satisfying any one of the following four conditions, the Eq. (1.3) has a smooth periodic wave solution as the form of the expression (2.16).

(1) $c > 0$, $0 \leq g < g_1$ and $-f_0(\varphi_-) < h < -f_0(\varphi_+)$.
(2) $c > 0$, $g_2 < g < 0$ and $-f_0(\varphi_-) < h < -f_0(\varphi_c)$.
(3) $c < 0$, $0 \leq g < g_1$ and $-f_0(\varphi_+) < h < -f_0(\varphi_-)$.
(4) $c < 0$, $g_2 < g < 0$ and $-f_0(\varphi_c) < h < -f_0(\varphi_+)$.

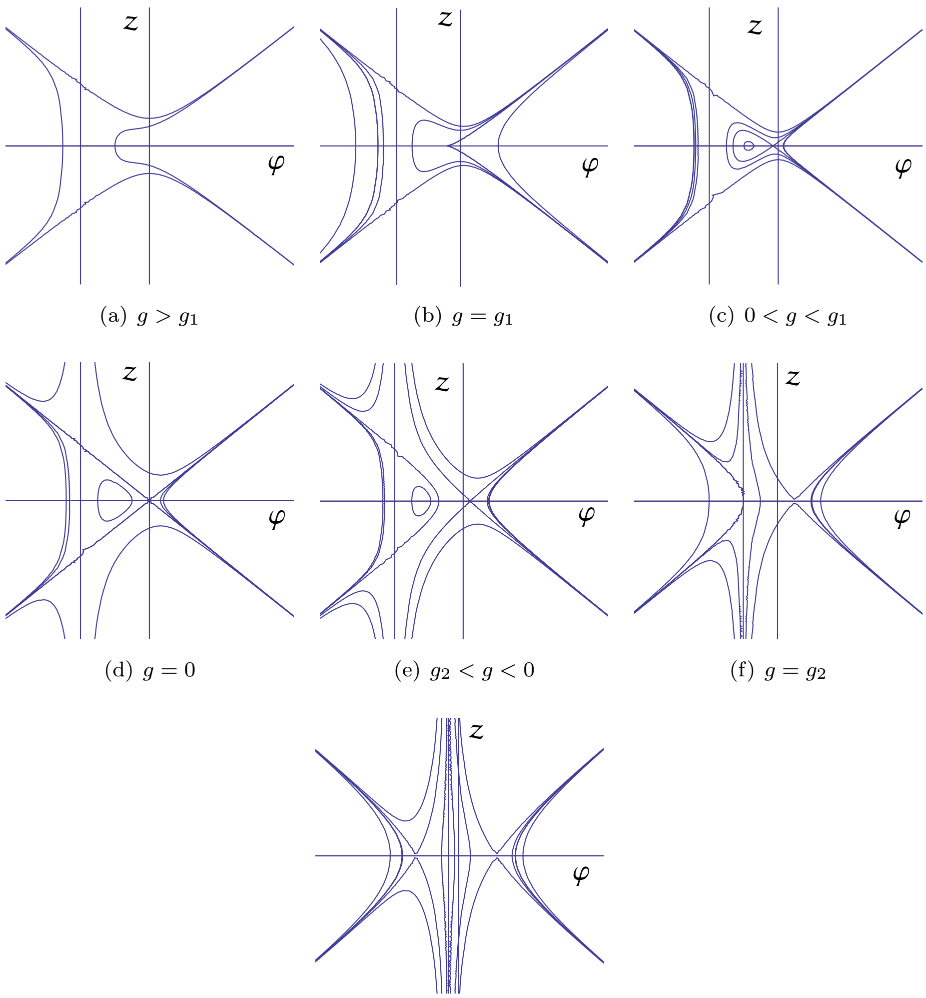

(a) $g > g_1$ (b) $g = g_1$ (c) $0 < g < g_1$

(d) $g = 0$ (e) $g_2 < g < 0$ (f) $g = g_2$

(g) $g < g_2$

Figure 1. The bifurcation phase portraits of system (3.1) with $c > 0$.

3.2. Periodic cusp waves

(a) When $c > 0$, $g_2 < g < 0$ and $h = -f_0(\varphi_c)$, by using solution (2.19), we obtain a periodic cusp wave solution of Eq. (1.3) as follows:

$$u(\xi) = \frac{1}{2}\left[\varphi_2 + \varphi_3 - (\varphi_3 - \varphi_2)\cosh(\xi - 2nT)\right], \text{ for } (2n-1)T < \xi \leq (2n+1)T, \tag{3.2}$$

where $n = 0, \pm 1, \pm 2, \cdots$, and $T = \int_{\varphi_c}^{\varphi_1} \frac{ds}{\sqrt{(\varphi_1 - s)(\varphi_2 - s)}} = 2\ln \frac{\sqrt{\varphi_2 - \varphi_1}}{\sqrt{\varphi_2 - \varphi_c} + \sqrt{\varphi_1 - \varphi_c}}$.

(b) When $c < 0$, $g_2 < g < 0$ and $h = -f_0(\varphi_c)$, by using solution (2.22), we obtain a periodic cusp wave solution of (1.3) as follows:

$$u(\xi) = \frac{1}{2}[\varphi_1 + \varphi_2 + (\varphi_2 - \varphi_1)\cosh(\xi - 2nT)], \text{ for } (2n-1)T < \xi \leq (2n+1)T, \tag{3.3}$$

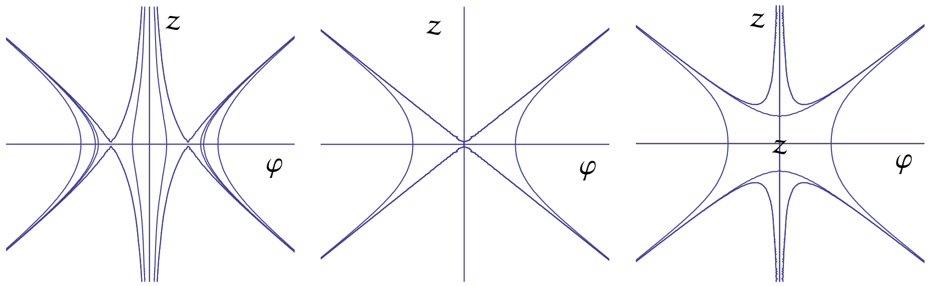

(a) $g < 0$ (b) $g = 0$ (c) $g > 0$

Figure 2. The bifurcation phase portraits of system (3.1) with $c = 0$.

where $n = 0, \pm 1, \pm 2, \cdots$, and $T = \int_{\varphi_2}^{\varphi_c} \frac{ds}{\sqrt{(s-\varphi_1)(s-\varphi_2)}} = 2 \ln \frac{\sqrt{\varphi_c - \varphi_1} + \sqrt{\varphi_c - \varphi_2}}{\sqrt{\varphi_2 - \varphi_1}}$.

3.3. Periodic loop waves

Satisfying any one of the following two conditions, the Eq. (1.3) has a periodic loop wave solution which is expressed by (2.16).
(1) $c \geq 0$, $g < g_2$ and $-f_0(\varphi_c) < -f_0(\varphi_-)$.
(2) $c < 0$, $g < g_2$ and $-f_0(\varphi_c) < -f_0(\varphi_+)$.

3.4. Solitary loop waves

1) If $0 < c$, $g < g_2$ and $h = -f_0(\varphi_-)$, then the Eq. (1.3) has a solitary loop wave solution which is expressed by (2.18).
2) If $c < 0$, $g < g_2$ and $h = -f_0(\varphi_+)$, then the Eq. (1.3) has a solitary loop wave solution which is expressed by (2.21).

3.5. Smooth solitary waves

(*1*) If $0 < c$, $0 < g < g_1$ and $h = -f_0(\varphi_+)$, then the Eq. (1.3) has a smooth solitary wave solution which is expressed by (2.21).
(*2*) If $c < 0$, $0 < g < g_1$ and $h = -f_0(\varphi_-)$, then the Eq. (1.3) has a smooth solitary wave solution which is expressed by (2.18).

3.6. Peakons

If $c \neq 0$, $g = 0$ and $h = 0$, then the Eq. (1.3) has a peakon solution which is expressed by (2.24).

3.7. Kink waves

If $c = 0$, $g < 0$ and $h = -f_0(\varphi_-) = -f_0(\varphi_+)$, then the Eq. (1.3) has two kink solutions $u_1(x,t) = \varphi(\xi)$, for $\frac{d\varphi}{d\xi} > 0$; $u_2(x,t) = \varphi(\xi)$, for $\frac{d\varphi}{d\xi} < 0$, where $\varphi(\xi)$ and ξ satisfy the equation (2.25).

Based on the above analysis, we will simulate the bounded travelling of Eq. (1.3) using mathematical software.

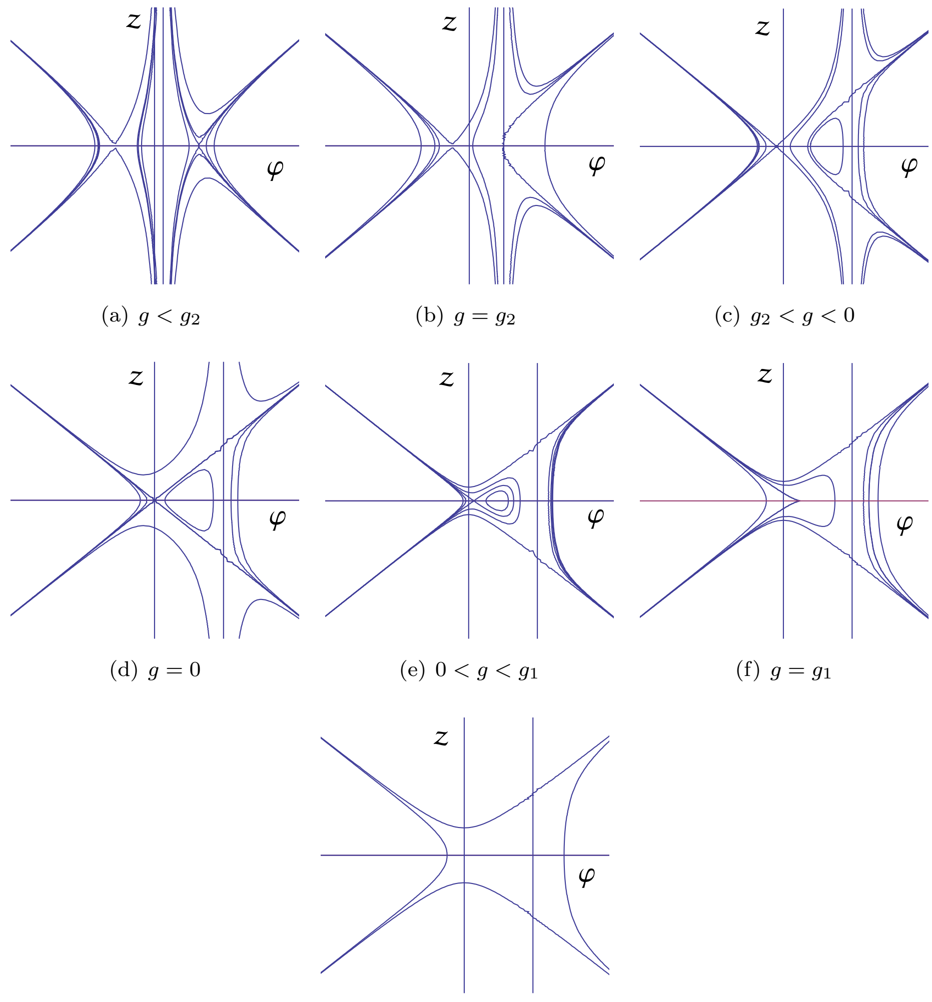

(a) $g < g_2$ (b) $g = g_2$ (c) $g_2 < g < 0$

(d) $g = 0$ (e) $0 < g < g_1$ (f) $g = g_1$

(g) $g_1 < g$

Figure 3. The bifurcation phase portraits of system (3.1) with $c < 0$.

Example 3.1. Choosing $c = 4$, then $g_1 = 1$ and $g_2 = -8$. We take $g = -2$, then $f_0(\varphi_c) = 16$, $f_0(\varphi_-) \approx 17.3923$ and $f_0(\varphi_+) \approx -3.3923$.

(1) Taking $h = -17$, we get $\varphi_1 = -2.2483$, $\varphi_2 \approx -1.59946$, $\varphi_3 \approx -1.16591$, $\varphi_4 \approx 1.01367$ and substituting these data into (2.16), we draw a graph of the profile of the smooth periodic wave solution which is shown in Fig. 4(a).

(2) Taking $h = -16$, we get $\varphi_1 = \varphi_c = -2$, $\varphi_2 = -1$, $\varphi_3 = 1$ and $T \approx 1.31696$ and substituting these data into (3.2), we draw a graph of the profile of the periodic cusp wave solution which is shown in Fig. 5(a).

Example 3.2. Choosing $c = -4$, then $g_1 = 1$ and $g_2 = -8$. We take $g = -2$, then $f_0(\varphi_c) = 16$, $f_0(\varphi_-) \approx -3.3923$ and $f_0(\varphi_+) \approx 17.3923$.

(1) Taking $h = -17$, we get $\varphi_1 = -1.01367$, $\varphi_2 \approx 1.16591$, $\varphi_3 \approx 1.59946$, $\varphi_4 \approx 2.2483$ and substituting these data into (2.16), we draw a graph of the profile

of the smooth periodic wave solution which is shown in Fig. 4(b).

(2) Taking $h = -16$, we get $\varphi_1 = -1$, $\varphi_2 = 1$, $\varphi_3 = \varphi_c = -2$ and $T \approx 1.31696$ and substituting these data into (3.3), we draw a graph of the profile of the periodic cusp wave solution which is shown in Fig. 5(b).

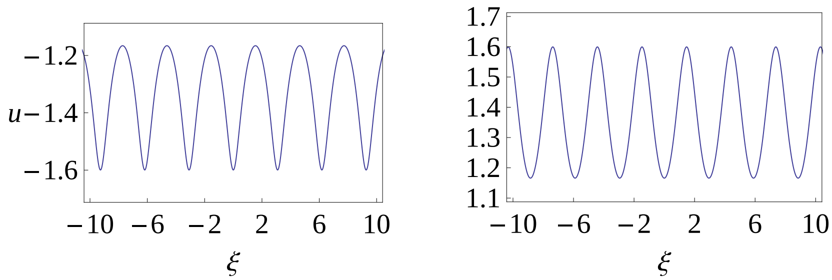

(a) $c = 4$ (b) $c = -4$

Figure 4. The smooth periodic waves of Eq. (1.3) with $g = -2$ and $h = -17$.

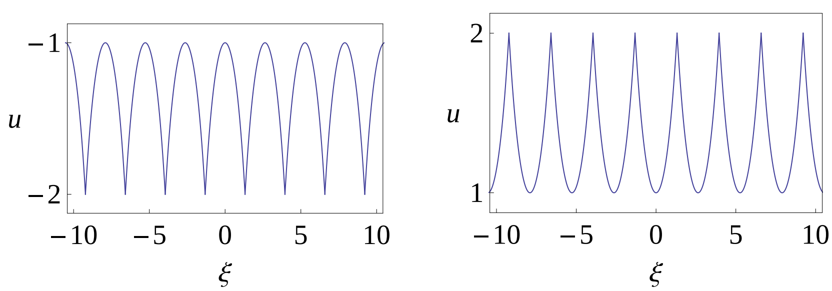

(a) $c = 4$ (b) $c = -4$

Figure 5. The periodic cusp waves of Eq. (1.3) with $g = -2$ and $h = -16$.

Example 3.3. Choosing $c = 4$, then $g_1 = 1$ and $g_2 = -8$. We take $g = -15$, then $f_0(\varphi_c) = 120$, $f_0(\varphi_-) = 118.75$ and $f_0(\varphi_+) = -137.25$.

(1) Taking $h = -119$, we get $\varphi_1 \approx -2.61526$, $\varphi_2 \approx -2.35977$, $\varphi_3 \approx -1.76155$, $\varphi_4 \approx 2.73658$. S and substituting these data into (2.16), we draw a graph of profile of the periodic loop wave which is shown in Fig. 6(a).

(2) Taking $h = -118.75$, we get $\varphi_1 = -2.5$, $\varphi_2 \approx -1.73607$, $\varphi_3 \approx 2.73607$ and substituting these data into (2.18), we draw a graph of profile of the solitary loop wave solution which is shown in Fig. 7(a).

Example 3.4. Choosing $c = -4$, then $g_1 = 1$ and $g_2 = -8$. We take $g = -15$, then $f_0(\varphi_c) = 120$, $f_0(\varphi_-) = -137.25$ and $f_0(\varphi_+) = 118.75$.

(1) Taking $h = -119$, we get $\varphi_1 \approx -2.73658$, $\varphi_2 \approx 1.76155$, $\varphi_3 \approx 2.35977$, $\varphi_4 \approx 2.61526$ and substituting these data into (2.16), we draw a graph of profile of the periodic loop wave solution which is shown in Fig. 6(b).

(2) Taking $h = -118.75$, we get $\varphi_1 \approx -2.73607$, $\varphi_2 \approx 1.73607$, $\varphi_3 = 2.5$. and substituting these data into (2.21), we draw a graph of profile of solitary loop wave solution which is shown Fig. 7(b).

Example 3.5. Choosing $c = 4$, then $g_1 = 1$ and $g_2 = -8$.

(1) We take $g = 0.5$, then $f_0(\varphi_c) = -4$, $f_0(\varphi_-) \approx 1.14461$ and $f_0(\varphi_+) \approx -0.269607$. Choosing $h = 0.269607$, we get $\varphi_1 \approx -2.39475$, $\varphi_2 \approx -1.31236$ and $\varphi_3 \approx -0.146447$. Substituting these data into (2.21), we draw a graph of profile of smooth solitary wave solution which is shown in Fig. 8(a).

(2) We take $g = 0$ and $h = 0$, then $\varphi_c = -2$. Substituting these data into (2.24), we draw graph of profile of a peakon solution which is shown in Fig. 9(a).

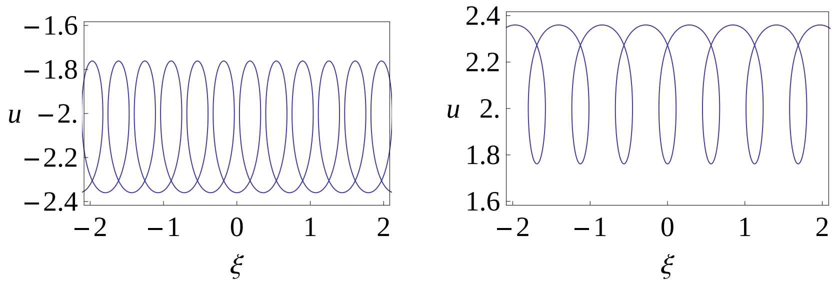

(a) $c = 4$ (b) $c = -4$

Figure 6. The periodic loop waves of Eq. (1.3) with $g = -15$ and $h = -119$.

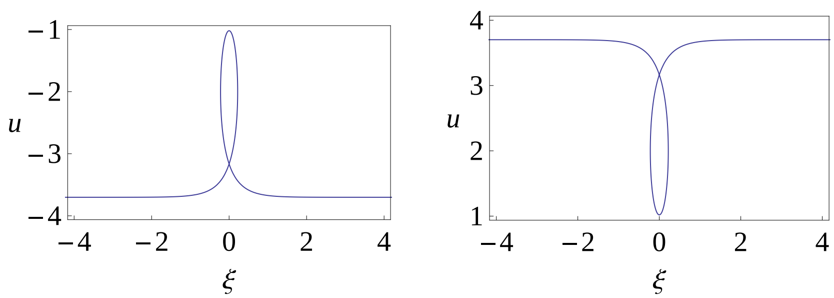

(a) $c = 4$ (b) $c = -4$

Figure 7. The solitary loop waves of Eq. (1.3) with $g = -15$ and $h = -118.75$.

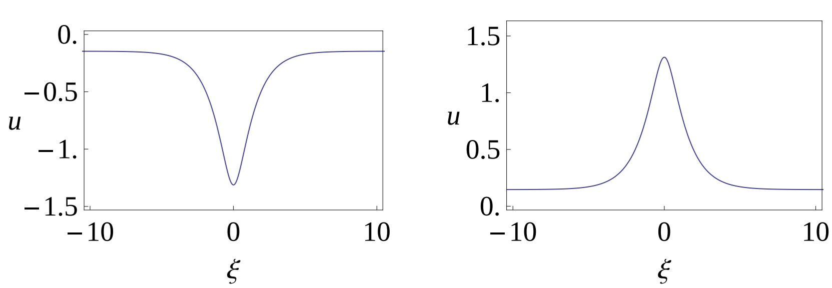

(a) $c = 4$ (b) $c = -4$

Figure 8. The solitary waves of Eq. (1.3) with $g = 0.5$ and $h = 0.269607$.

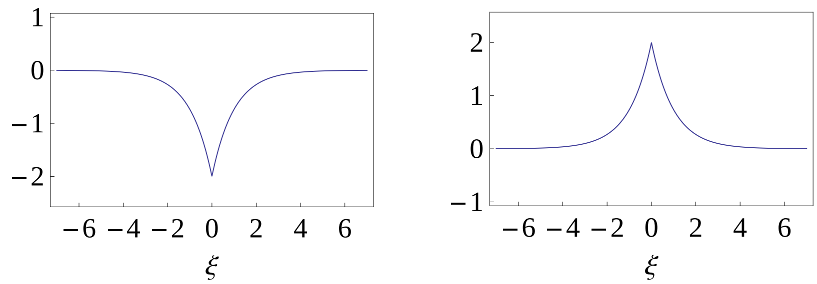

(a) $c = 4$ (b) $c = -4$

Figure 9. The peakons of Eq. (1.3) with $g = 0$ and $h = 0$.

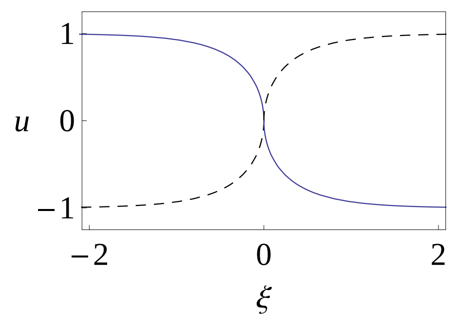

Figure 10. The kink waves of Eq. (1.3) with $c = 0$, $g = -4$, and $h = 4$.

Example 3.6. Choosing $c = -4$, then $g_1 = 1$ and $g_2 = -8$.

(1) We take $g = 0.5$, then $f_0(\varphi_c) = -4$, $f_0(\varphi_-) \approx -0.269607$ and $f_0(\varphi_+) \approx 1.14461$. Choosing $h = 0.269607$, we get $\varphi_1 \approx 0.146447$, $\varphi_2 \approx 1.31236$ and $\varphi_3 \approx 2.39475$. Substituting these data into (2.18), we draw a graph of profile of smooth solitary wave solution which is shown in Fig. 8(b).

(2) We take $g = 0$ and $h = 0$, then $\varphi_c = 2$. Substituting these data into (2.24), we draw a graph of profile of peakon solution of Fig. 9(b).

Example 3.7. Choosing $c = 0$, then $g_1 = g_2 = 0$. We take $g = -4$, then $f_0(\varphi_-) = f_0(\varphi_+) = -4$. Choosing $h = 4$, we get $\varphi_- = -1$ and $\varphi_+ = 1$. Substituting these data into (2.25), we draw two graphs of profile of kink solitary waves solutions which is shown in Fig. 10.

4. Conclusions

In this study, by using the planar bifurcation method of dynamical system, the gCH equation (1.3) have been studied, the periodic waves, periodic cusp waves, solitary waves, peakons, loops and kink waves, and their representations are obtained. We obtain classifications of travelling wave solutions of (1.3) and make numerical simulations of some bounded travelling wave by using mathematical software. The dynamical properties of these bounded travelling wave solutions mentioned above are simulated under the some parametric conditions (see Figs. 4–10).

Among these solutions obtained in this study, some of them have direct physical applications. For example, using the smooth solitary wave solutions, non-smooth peakon wave solutions, and kink and anti-kink wave solutions, loop wave and periodic loop wave solutions, we can explain lots of motion phenomena for water wave. For examples, the smooth solitary wave can be used to describe the motion phenomenon of a pile of water, loop wave can be used to describe the motion phenomenon of a turnup water wave.

References

[1] A. Bressan and A. Constantin, *Global conservative solutions of the Camassa-Holm equation*, Arch. Rational Mech., 183(2007)(2), 215–239.

[2] S. S. Behzadi, *Numerical solution of fuzzy Camassa-Holm equation by using homotopy analysis methods*, Journal of Applied Analysis and Computation, 1(2011)(3), 315–323.

[3] P. F. Byrd and M. D. Friedman, *Handbook of elliptic integrals for engineers and scientists*, Berlin: Springer, 1971.

[4] R. Camassa and D. Holm, *An integrable shallow water equation with peaked solitons*, Phys. Rev. Lett., 71(1993)(11), 1661–1664.

[5] R. Camassa, D. Holm and J. Hyman, *A new integrable shallow water equation*, Adv. Appl. Mech., 31(1994), 1–33.

[6] G. M. Coclite, F. Gargano and V. Sciacca, *Analytic solutions and singularity formation for the Peakon b-family equations*, Acta Appl. Math., 122(2012), 419–434.

[7] A. Degasperis, D. D. Holm and A. N. W. Hone, *A new integrable equation with peakon solutions*, Theor. Math. Phys., 133(2002)(2), 1463–1474.

[8] H. Holden and X. Raynaud, *Dissipative solutions for the Camassa-Holm equation*, Discrete Cont. Dyn. S., 24(2009)(4), 1047–1112.

[9] R. S. Johnson, *Camassa-Holm, Korteweg-de Vries and related models for water waves*, J. Fluid Mech., 455(2002), 63–82.

[10] R. S. Johnson, *On the solutions of the Camassa-Holm equation*, Proc. R. Soc. Lond. A, 459(2003)(2035), 1687–1708.

[11] J. Li and Z. Liu, *Smooth and non-smooth traveling waves in a nonlinearly dispersive equation*, Applied Mathematical Modelling, 25(2000)(1), 41–56.

[12] J. Li and Z. Liu, *Traveling wave solutions for a class of nonlinear dispersive equations*, Chinese Annals of Mathematics, 23(2002)(3), 397–418.

[13] M. C. Lombardo, M. Sammartino and V. Sciacca, *A note on the analytic solutions of the Camassa-Holm equation*, Comp. Rend. Math., 341(2005)(11), 659–664.

[14] T. Matsuo, *A Hamiltonian-conserving Galerkin scheme for the Camassa-Holm equation*, J. Comp. Appl. Math., 234(2010)(4), 1258–1266.

[15] A. V. Mikhailov and V. S. Novikov, *Perturbative symmetry approach*, J. Phys. A, 35(2002)(22), 4775–4790.

[16] A. B. De Monvel, A. Its and D. Shepelsky, *Painlev'e-type asymptotics for the Camassa-Holm equation*, SIAM J. Math. Anal., 42(2010)(4), 1854–1873.

[17] A. B. De Monvel, A. Kostenko, D. Shepelsky and G. Teschlh, *Long-time asymptotics for the Camassa-Holm equation*, SIAM J. Math. Anal., 41(2009)(4), 1559–1588.

[18] V. Novikov, *Generalization of the Camassa-Holm equation*, J. Phys. A, 42(2009), 342002-1-14.

[19] T. Rehman, G. Gambino and S. R. Choudhury, *Smooth and non-smooth traveling wave solutions of some generalized Camassa-Holm equations*, Commun. Nonlinear Sci. Numer. Simul., 19(2014)(6), 1746–1769.

[20] G. D. Rocca, M. C. Lombardo, M. Sammartino and V. Sciacca, *Singularity tracking for Camassa-Holm and Prandtl's equations*, Appl. Num. Math., 56(2006)(8), 1108–1122.

[21] A. M. Wazwaz, *Peakons, kinks, compactons and solitary patterns solutions for a family of Camassa-Holm equations by using new hyperbolic schemes*, Appl. Math. Comput., 182(2006)(1), 412–424.

[22] S. Xie and L. Wang, *Compacton and generalized kink wave solutions of the CH-DP equation*, Appl. Math. Comput., 215(2010)(11), 4028–4039.

[23] S. Xie, L. Wang and Y. Zhang, *Explicit and implicit solutions of a generalized Camassa-Holm-Kadomtsev-Petviashvili equation*, Commun. Nonlinear Sci. Numer. Simul., 17(2012)(3), 1130–1141.